Research Article

SURFACE and INTERFACE ANALYSIS

Received: 4 March 2010 Revised: 10 July 2010 Accepted: 21 July 2010 Published online in Wiley Online Library:

(wileyonlinelibrary.com) DOI 10.1002/sia.3684

Functionalized imidazolium wear-resistant ionic liquid ultrathin films for MEMS/NEMS applications

Yufei Mo,[a]* Fuchuan Huang[a] and Fei Zhao[b]

As a kind of new material, ionic liquids (ILs) are considered a new type of lubricant for micro/nanoelectromechanical system (M/NEMS) due to their excellent thermal and electrical conductivity. However, so far, only a few reports have investigated the friction and wear of thin films of these materials at the micro scale. Evaluating the nanoscale tribological performance of ILs when applied as films of a few nanometers thickness on a substrate is a critical step for their application in M/NEMS devices. To achieve this purpose, IL thin films with four kinds of anions were synthesized and prepared on single-crystal silicon wafers by the dip-coating method. Film thickness was determined by the ellipsometric method. Their surface morphologies were observed by means of atomic force microscopy (AFM). The nano and micro tribological properties of the IL films were investigated by a friction force microscope (FFM)with a spherical probe and a UMT-2MT tribotester, respectively. The corresponding morphologies of the wear tracks of the IL films were examined using a three-dimensional non-contact interferometric microscope. The impact of temperature on the adhesion behavior was studied, as well as the effect of sliding frequency and load on the friction coefficient, load bearing capacity and anti-wear durability. It was found that friction, adhesion and durability of IL films were strongly dependent on their anionic molecular structures, wettability and ambient environment.

Keywords: ionic liquid; ultrathin film; atomic force microscopy; adhesion; wear

Introduction

Micro/nanoelectromechanical systems (M/NEMS) have been developed in recent years following the improvements in nanotechnology.[1] The commercialization of products based on M/NEMS relies on a better understanding of the various devices. Adhesion and friction at the nanometer scale becomes critical and can be detrimental to the efficiency, power output and reliability of MEMS/NEMS devices.[2] For example, adhesion is a major cause of failure of accelerometers used in automobile air-bag triggering mechanisms[3] and in digital micromirror displays.[4] In order to improve tribological performance, lubricants are applied to the M/NEMS device surfaces. The ideal lubricant should be molecularly thick, easy to be applied, highly durable and insensitive to the environment.[5]

Over the past years, many molecular thin films have been studied, such as fatty acids, silanes, thiols, phospholipids and polymeric films.[6–8] These films can provide load-supporting strength owing to high packing density and solid-state-like properties. However, these monolayer films do not last long under repeated sliding. When some of molecules are removed from the surface by mechanical rubbing, the films tend to fracture and break down.[9,10]

It is generally accepted that ionic liquids (ILs) are molten salts with a melting point below 100 °C. Room-temperature ionic liquids (RTILs) are synthetic salts with melting points at or below room temperature. They are composed of ion pairs containing bulky asymmetric cations and anions. At least one ion has a delocalized charge such that the formation of a stable crystal lattice is prevented and ions are held together by strong electrostatic forces. Imidazolium, pyridinium, ammonium and phosphonium are the mostly frequently used cations. The anions are categorized into hydrophobic anions with weak hydration capacity, and hydrophilic ones. ILs possess a combination of unique characteristics, including negligible volatility, non-flammability, high thermal ability, low melting point and conductivity. These have motivated research and led to various applications in many fields, for example as electrolytes in batteries and for electrodeposition, and as green solvents for a wide range of organic synthesis, catalysis, electrochemistry, and photochemistry, and so on.[11–23]

On the other hand, the unique characteristics of ILs are also just what high-performance lubricants demand in M/NEMS. Their strong electrostatic bonding compared to covalently bonded fluids leads to very desirable lubrication properties. Unlike conventional lubricants that are electrically insulating, ILs can minimize the contact resistance between sliding surfaces because they are conductive, and conductive lubricants are needed for various electrical applications.[24] In addition, ILs have high thermal conductivities, which help dissipate heat during sliding.[25] The use of ILs instead of hydrocarbon-based oil has the potential to dramatically reduce air-polluting emissions. In very harsh friction conditions, lubricants are required to have high thermal stability and chemical inertness. Perfluoropolyethers (PFPEs) have been

* *Correspondence to: Yufei Mo, School of Chemistry and Chemical Engineering, Guangxi University, Nanning 530004, P. R. China. E-mail: yufeimo@gxu.edu.cn*

a *School of Chemistry and Chemical Engineering, Guangxi University, Nanning 530004, P. R. China*

b *School of Materials Science and Engineering, Henan University of Science and Technology, Luoyang 471003, P. R. China*

used in magnetic rigid disk and vacuum grease applications in the past decades due to their high thermal stability and extremely low vapor pressure.[26] However, PFPEs often go out of action due to degradation catalyzed by strong nucleophilic agents and strong electropositive metals,[27,28] which together with their high cost can limit their application in many fields. The decomposition temperatures of imidazolium ILs are generally above 300 °C, which, together with the low temperature fluidity and glass transition temperature below −50 °C, means that ILs can function over a wide temperature range. The most notable characteristic that distinguishes ILs from other synthetic lubricants is its high polarity.[29] The high polarity of ILs enables them to form very strong and effective adsorption films, which contribute to their prominent anti-wear capability.

In this study, atomic force microscopy (AFM)-based adhesion and friction measurements are presented for silicon substrates coated with some ILs of interest. A friction force microscope (FFM) was employed to investigate the interfacial structure and tribological properties of IL thin films. A homemade spherical probe was used instead of the normal silicon nitride probes to reduce the contact pressures produced by sharper silicon nitride tips. Conventional ball-on-flat data are used in conjunction with FFM experiments to compare the friction and wear properties at the micro and nano scale.

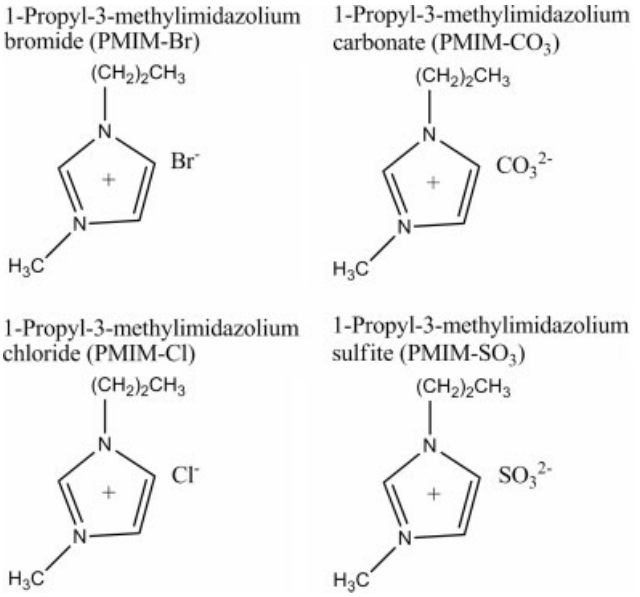

Figure 1. Molecular structures of PMIM-Br, PMIM-CO_3, PMIM-Cl and PMIM-SO_3 molecules.

Experimental

Materials and sample preparation

Polished and cleaned single-crystal silicon (100, p-doped) wafers, obtained from GRINM Semiconductor Materials Co., Ltd. Beijing, were used as substrates for all the data presented in this work. Silicon substrates with dimensions $10 \times 10 \times 0.5$ mm were cut from Si wafers. The wafers were ultrasonicated in acetone followed by isopropanol for 5 min each. They were then treated in a fleshly prepared Piranha solution (volume ratio 7 : 3 of 98% H_2SO_4 and 30% H_2O_2) at 90 °C for 30 min to get a hydroxyl-terminated surface.

The ILs used in this study are 1-propyl-3-methylimidazolium bromide, 1-propyl-3-methylimidazolium carbonate, 1-propyl-3-methylimidazolium chloride and 1-propyl-3-methylimidazolium sulfite abbreviated as PMIM-Br, PMIM-CO_3, PMIM-CL and PMIM-SO_3, respectively. Their molecular structures are schematically shown in Fig. 1. The lubricants were applied on single-crystal silicon using the dip-coating technique. The dip-coating procedure is as follows. The silicon wafers were pulled from the solution with the aid of the motorized stage set at a constant speed of 60 μm/s to obtain films of the desired thickness. The solution of ILs in ethanol with an appropriate concentration was dip-coated onto pretreated silicon substrates and then dried at 90 °C for 10 min. The thicknesses of the films after dip-coating were measured by the ellipsometric method. All procedures were carried out in a class-10 clean room at a relative humidity (RH) of 15% and temperature of 20 °C.

Nanoscale adhesion and friction measurements

Adhesion and friction force measurements were carried out using a commercial CSPM 4000 AFM/FFM microscope under ambient conditions (20 °C, 15% RH). A colloidal probe was prepared by gluing a glass sphere with a radius of 37.5 μm onto a tipless cantilever (normal force constant 2 N/m). The colloidal probe is shown in Fig. 2. The colloidal probe was

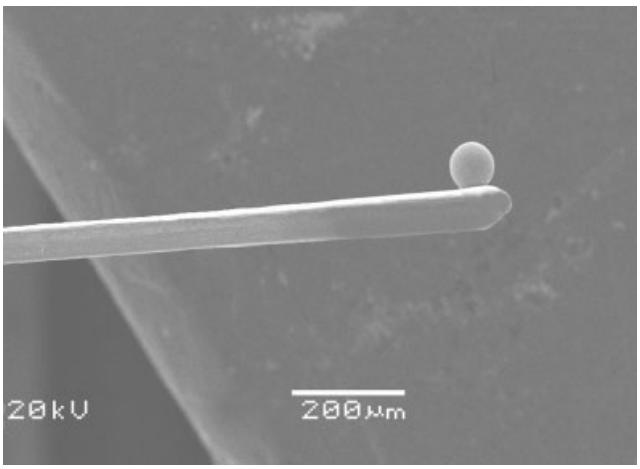

Figure 2. SEM image of the colloidal probe.

cleaned by ethanol and acetone in turn before use. For all experiments, the same cantilever was used in this comparative study. Furthermore, to avoid the influence of molecules that may be transferred to tip on the FFM probe, the colloidal probe was scanned on a cleaved mica surface to remove physically adsorbed molecules. The surface topography of the colloidal probe was scanned with a cantilever of force constant 0.12 N/m and a sharp silicon nitride tip in the contact mode, as shown in Fig. 3. The RH was controlled at 15%. Repeated measurements were within 5% of the average value for each sample.

Commercially available rectangular Si_3N_4 cantilevers with normal force constant of 0.4 N/m, radius of about 10 nm and back-coated by gold (Budgetsensors Instruments, Inc.) were employed. The force–distance curves were recorded, and the pull-off force was taken as the adhesive force given by $F = K_c Z_p$, Where K_c is the force constant of the cantilever and Z_p is the

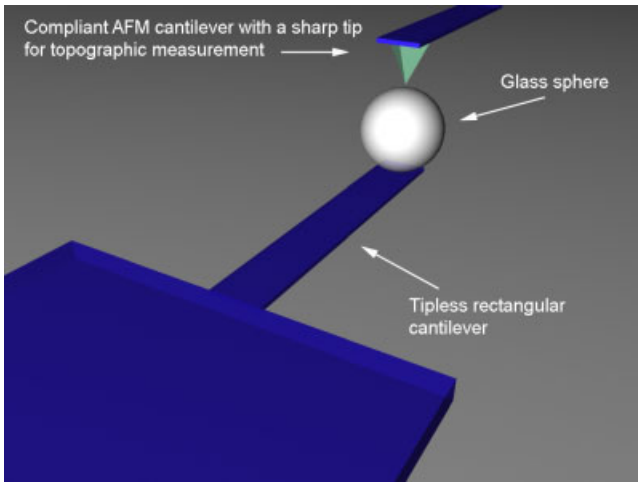

Figure 3. Schematic illustration on topographic measurement of the colloidal probe.

vertical displacement of the piezotube, i.e. the deflection of the cantilever.[30–33]

The frictional force is the lateral force exerted on the tip during scanning and can be measured using the twist of the tip/cantilever assembly. To obtain frictional data, the tip was scanned back and forth in the *x* direction in contact with sample at a constant load while the lateral deflection of the lever was measured. The difference in the lateral deflection or frictional signal between back and forth motions is proportional to the frictional force. The frictional force was calibrated by the method described in the Ref. [34]. Frictional forces were continuously measured with various external loads. The load was increased (or decreased) linearly in each successive scan line. Scanning for the frictional force measurement was performed at rate of 1 Hz along the scan axis and at a scan size of 50 µm × 50 µm (*viz.* sliding velocity of 100 µm/s). The scan axis was perpendicular to the longitudinal direction of the cantilever. The sets of data were displayed graphically in a friction image.

Microscale friction and wear measurements

The friction coefficient and durability at the microscale were evaluated using a pin-on-plate tribometer in the reciprocating mode. A Si_3N_4 ball of 3.18 mm diameter was fixed on a stationary holder supported by a beam and the samples were then mounted on a reciprocating table. The ball moved horizontally with respect to the sample surface with a sliding frequency between 1 and 20 Hz and a travel of 5 mm. The applied normal loads were between 60 and 300 mN and the change in the friction coefficient was monitored *versus* sliding times or cycles. The initiation of wear on the sample surface leads to an increase in the friction coefficient, and a sharp increase indicates the failure of the film. The friction coefficient and sliding cycles were recorded automatically by a computer. A schematic illustration of ball-on-plate tribometer is showed in Fig. 4. All the tests were conducted at room temperature and an RH of 15%.

The worn surfaces of the films were observed on a MicroXAM 3D non-contact interferometric microscope (ADE Phase Shift, Inc., USA) in the phase mode.

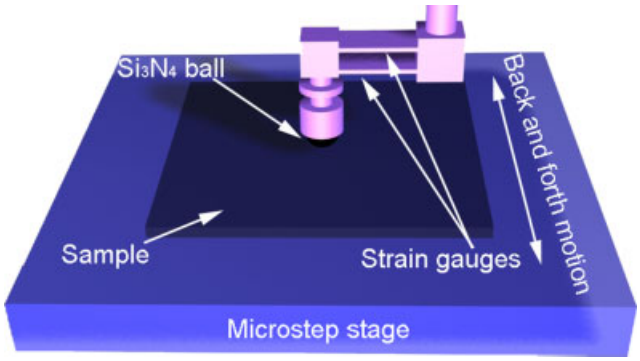

Figure 4. Schematic illustration of pin-on-plate tribometer.

Results and Discussion

Characterization of ILand films

The thermal properties of four kinds of ILs were examined on a TGA-7 thermogravimetric analyzer (Perkin-Elmer, USA) between 20 and 600 °C with a heating rate of 10 °C/min. As shown in Fig. 5, All the ILs exhibited high decomposition temperatures, assigned to 250, 260, 280 and 320 °C, respectively.

Figure 6 shows the plots of film thickness as function of the IL solution concentration. The data indicate that the linear increase in film thickness is associated with the increase of the solution concentration. According to this relationship, a film of the desired thickness was easily prepared.

Figure 7(a) and (b) shows the AFM topographies of the Si surface before and after the dip-coating treatment in the IL solution. Figure 7(a) shows that hydroxylated Si surface is smooth and uniform with a root-mean-square (rms) roughness of about 0.1 nm. The surface topography of the PMIM-Cl IL film is shown in Fig. 7(b). It is observed that the films were homogenously distributed on the silicon surface with the rms roughness of about 0.4 nm.

Nanotribological behavior

Adhesion is generally measured by the amount of force necessary to separate two surfaces in contact. At the nanoscale, mechanical loading is often not the overwhelming force as in the macroscale, and surface forces such as van der Waals, electronic and

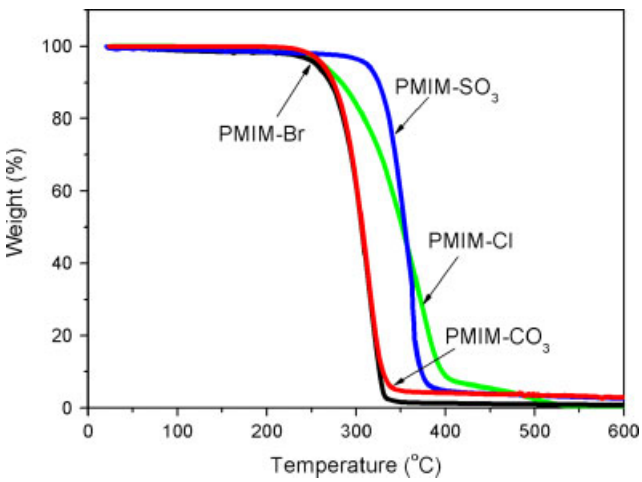

Figure 5. TGA curves of PMIM-Br, PMIM-CO_3, PMIM-Cl and PMIM-SO_3 ILs.

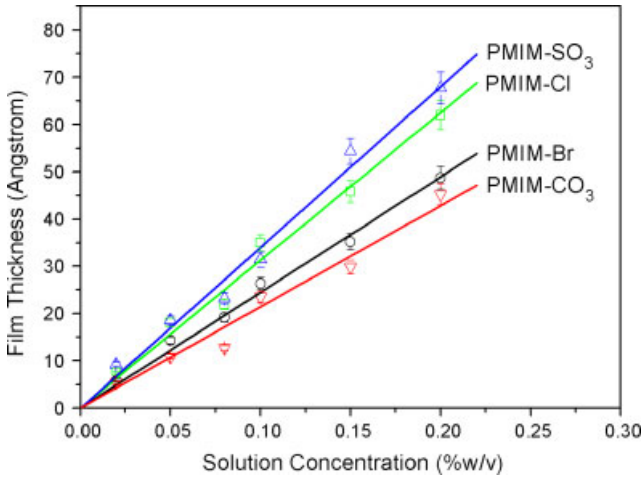

Figure 6. Plot of film thickness as function of the IL solution concentration at a pull-off velocity of 60 μm/s.

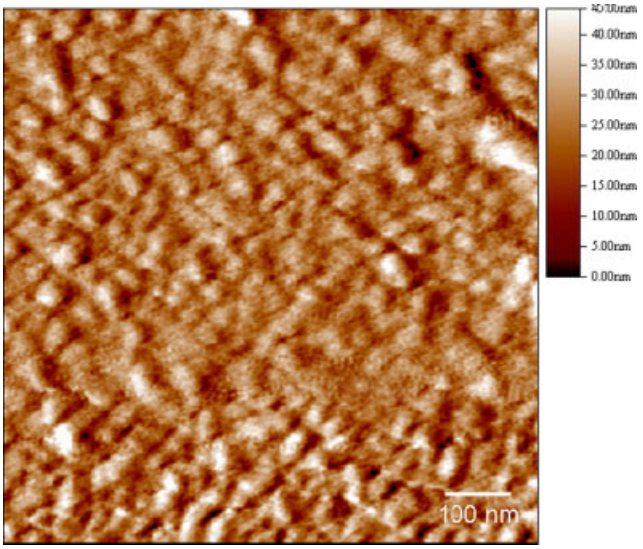

Figure 8. AFM topographic image of the tip surface of the colloidal probe.

capillary/meniscus forces become significant in controlling the pull-off force. Figure 8 shows the three-dimensional (3D) surface topography of a colloidal probe. The microroughness of the colloidal probe in terms of the rms of the monolayer was estimated to be 7.5 nm over an area of 1 μm × 1 μm (512 × 512 resolution).

The adhesive forces between the AFM spherical tip and the IL film surfaces are shown in Fig. 9. The Si substrate data are provided for comparison. A strong adhesive force of about 184 nN was observed on the hydroxylated Si surface at an RH of 15%. After the ILs were coated, the adhesive force decreased to 90, 142, 121 and 88 nN, respectively. The adhesive force was observed to decrease in the following order: PMIM-CO_3 >PMIM-Br>PMIM-CL>PMIMCH-SO_3. The hydrophilic property of the anionic groups in the IL films facilitates the formation of a meniscus, which increases the tip–sample adhesion. The adhesive force is the lowest in PMIMCH-SO_3 since it has the greatest amount of relative hydrophobic anionic groups among the four IL samples.

Figure 10 presents the plot of friction *versus* load curves for the hydroxylated Si surface and the IL films. It is observed that the IL films greatly reduced the friction force, and especially the

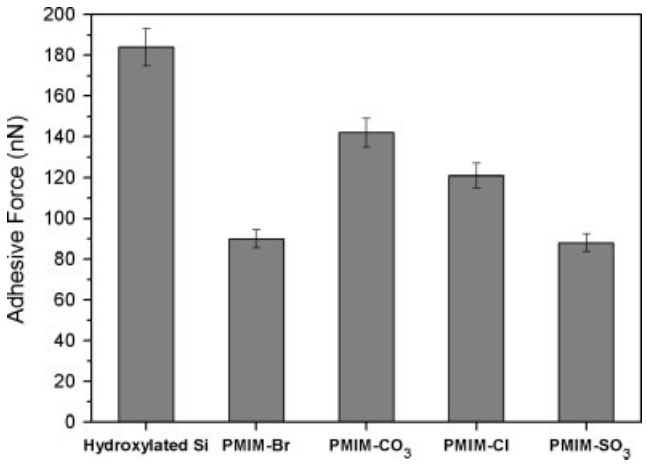

Figure 9. Adhesive forces between colloidal probe and the surfaces of PMIM-Br, PMIM-CO_3, PMIM-Cl and PMIM-SO_3 IL films at an RH of 15%.

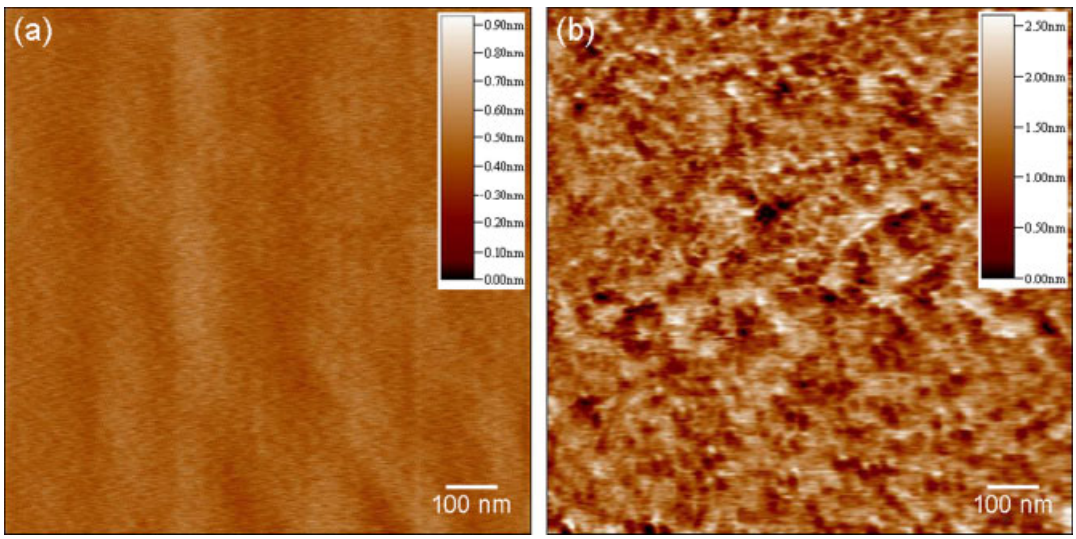

Figure 7. AFM images of for hydroxylated Si (a) and PMIM-Cl (b) IL film surfaces.

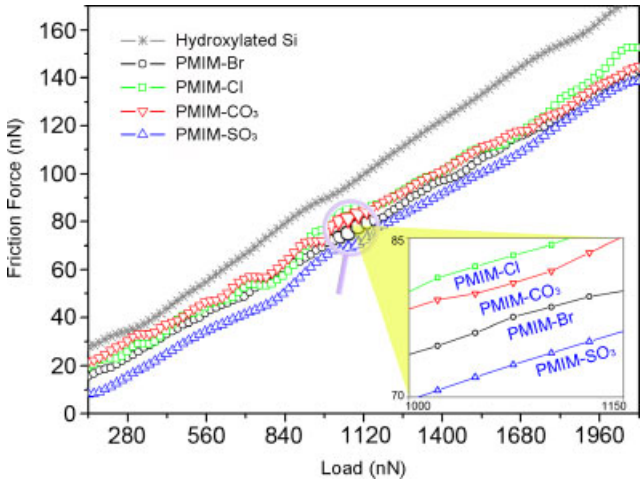

Figure 10. Plot of friction and load for surfaces of hydroxylated Si, PMIM-Br, PMIM-CO_3, PMIM-Cl and PMIM-SO_3 at an RH of 15%.

PMIMCH-SO_3 exhibited the lowest friction. The results imply that the hydrophilic property of the anionic group samples facilitated sliding of the spherical tip on the surface. However, the values of friction for PMIM-CO_3, PMIM-Br and PMIM-Cl are higher than for PMIMCH-SO_3. This is because the water and lubricant molecules are more likely to form a meniscus as the spherical tip approaches the surface. This provides greater resistance to tip sliding, leading to higher values of friction.

Microtribological behavior

The tribological performance was evaluated for the hydroxylated Si substrate and the IL-coated surfaces with film thickness of about 2 nm. Without the protection of the IL films, the coefficient of friction of the hydroxylated Si substrate increased sharply and was stable at a constant value of about 0.65.

In order to compare friction and wear properties, conventional ball-on-plate tribometer experiments were conducted on the same samples. Figure 11(a)–(d) contains plots of the coefficient of friction as a function of the number of sliding cycles at normal loads ranging from 60 to 300 mN. As shown in Fig. 11(a), the friction coefficient of PMIM-Br was 0.15 at the normal load of 60 mN. When the normal load rose to 100 mN, the friction coefficient rose sharply to over 0.65 before reaching 2800 cycles, implying that the lubricant film failed. The friction coefficients of PMIM-CO_3 averaged at 0.14 and 0.16 at normal loads of 60 and 100 mN, respectively, as shown in Fig. 11(b). The PMIM-CO_3 film failed at

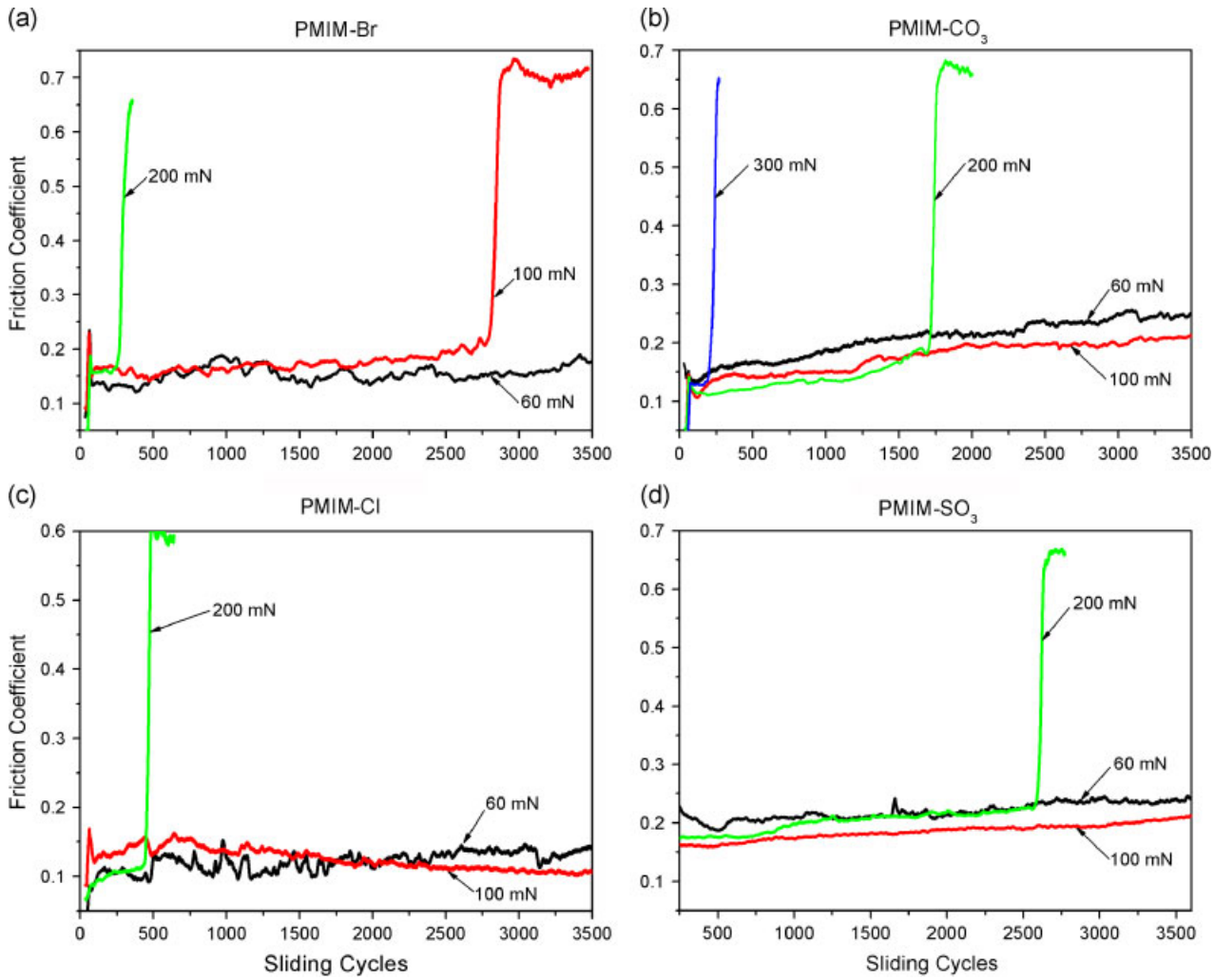

Figure 11. Plots of friction coefficients as function of sliding cycles for PMIM-Br (a), PMIMOH-CO_3 (b), PMIM-Cl (c) and PMIM-SO_3 (d) film on silicon.

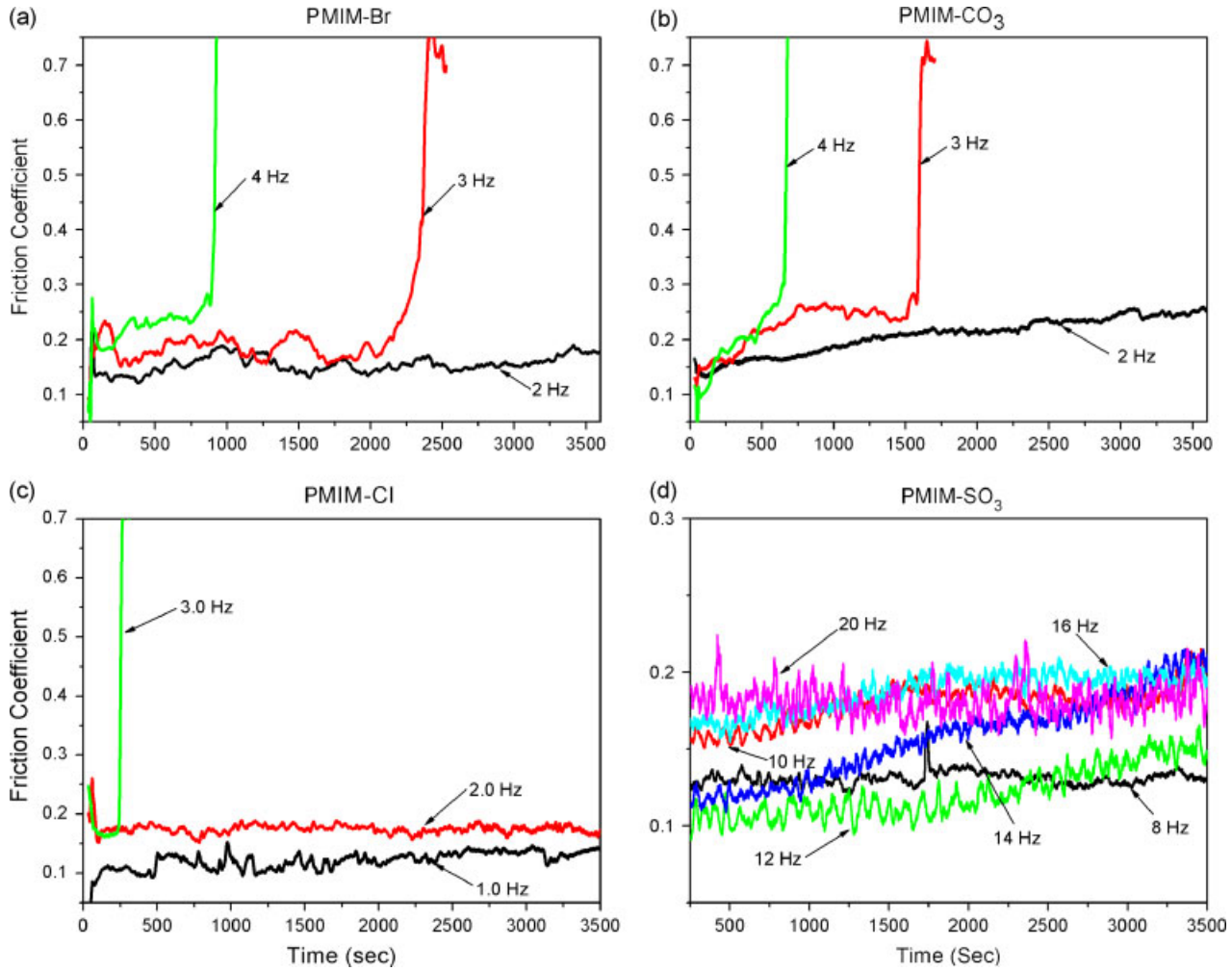

Figure 12. Plots of friction coefficients as function of sliding frequency for PMIMCH-Br (a), PMIM-CO_3 (b), PMIM-Cl (c) and PMIM-SO_3 (d) films at a normal load of 60 mN.

the normal load of 200 mN. As shown in Fig. 11(c) and (d), the friction coefficient of PMIM-CL and PMIM-SO_3 averaged at 0.12 and 0.18 at all loads, and failed at a load of 200 mN. Only a small rise in the coefficient of friction was observed for both PMIM-CO_3 and PMIM-SO_3 surface below the load of 200 mN, indicating a low surface wear. However, both PMIM-CO_3 and PMIM-SO_3 samples exhibited a gradual change in the value of the friction coefficient. This is attributed to the transfer of lubricant molecules to the Si_3N_4 ball and the interaction of the transferred molecules with the lubricant still attached to the Si surface, which increase the frictional force.

Figure 12(a)–(d) shows the effect of the sliding frequency on the coefficient of friction for all IL films at a normal load of 60 mN. As shown in Fig. 12(a)–(c), the friction coefficient of PMIM-Br, PMIM-CO_3 and PMIM-Cl averaged about 0.14, 0.19, 0.13 at relatively mild conditions (below 2 Hz). When the sliding frequency rose to 3 Hz, their friction coefficient sharply increased to over 0.6 in tens of minutes, which indicated that the IL films failed completely under the higher frequency reciprocating movement. At the same time, the PMIM-SO_3 still maintained a low friction coefficient of 0.12, 0.13 and 0.14 under high frequencies of 8, 12 and 14 Hz, as shown in Fig. 12(d). Even at the severe condition of 20 Hz, the PMIM-SO_3 possessed a low friction coefficient and long durability.

To further clarify the friction behavior, 3D interferometric microscope images and cross-section maps of the wear tracks are shown in Fig. 13. Figure 13(a) shows the worn surfaces and cross-section maps of PMIM-Br, PMIM-CO_3, PMIM-Cl and PMIM-SO_3 films at various normal loads and a frequency of 1 Hz (*viz.* velocity of 10 mm/s) after sliding against the Si_3N_4 ball for 3600 cycles. Figure 13(b) shows the morphology of the worn surface and the cross-section maps of the Si substrate coated with PMIM-Br, PMIM-CO_3, PMIM-Cl and PMIM-SO_3 at various frequencies and normal load of 60 mN after sliding against the Si_3N_4 ball for 3600s. Figure 13(c) shows morphology and cross-section maps of the worn surface of bare Si at various frequencies and a normal load of 60 mN for 1000 s. In all cases, IL-coved Si exhibits a smaller amount of debris and less wear compared to the uncoated Si surface, indicating that IL films provide wear protection. As shown in Fig. 13(a) and (b), it is observed that some regions of the wear tracks are filled with the lubricant, especially at lower loads and frequencies, which does not occur in the uncoated Si (Fig. 13(c)). The IL-coated Si surface exhibits low-wear surfaces, which is attributed to lubricant replenishment by the mobile fraction.

Figure 14(a) shows 3D interferometric microscope images of worn surface of the counterpart ball against various films at loads of 60 mN and frequency of 3 Hz for 3600 s. Figure 14(b) presents

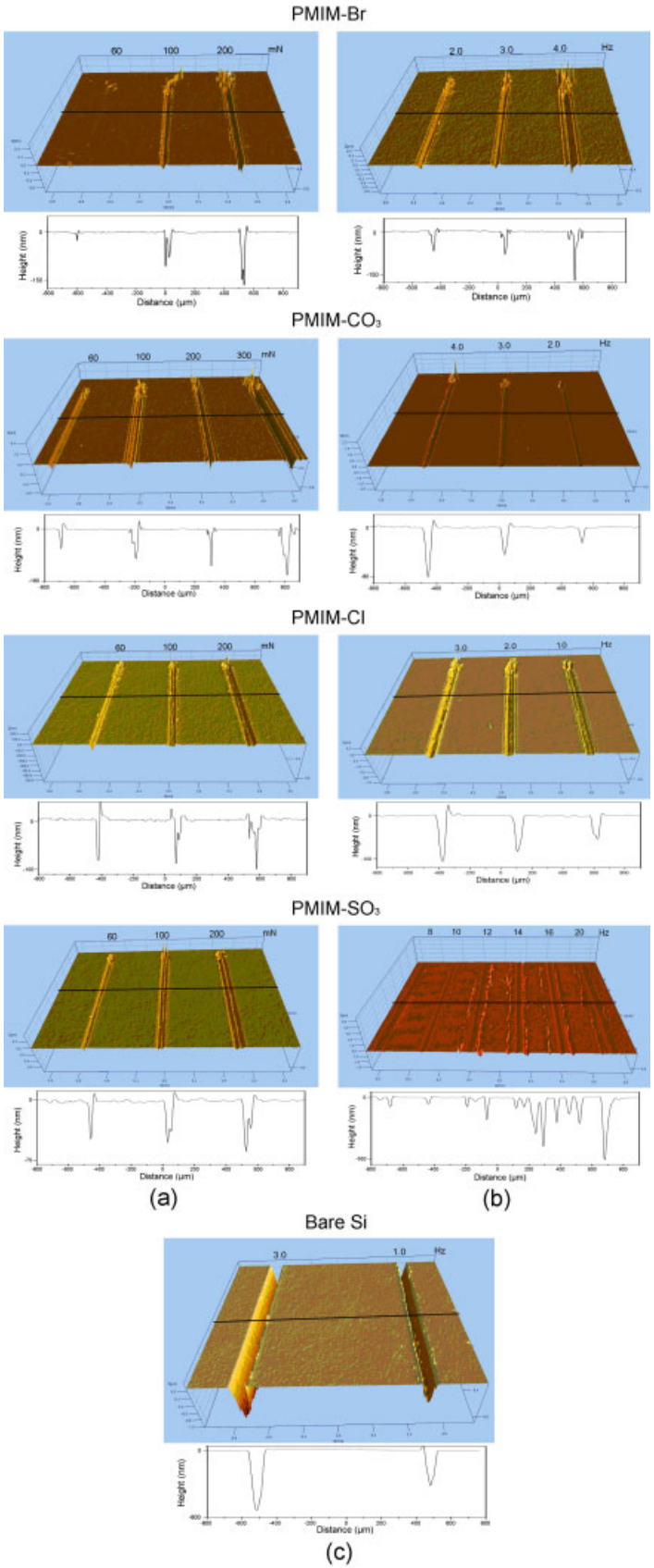

Figure 13. Three-dimensional interferometric microscope images and cross-section maps of the wear tracks of PMIMCH-Br, PMIM-CO_3, PMIM-Cl and PMIM-SO_3 films after wear test at various normal loads and a frequency of 1 Hz for 3600 cycles (a); at various frequencies and normal load of 60 mN for 3600 s (b); bare Si at load of 60 mN and frequencies of 1 and 3 Hz for 1000 s (c).

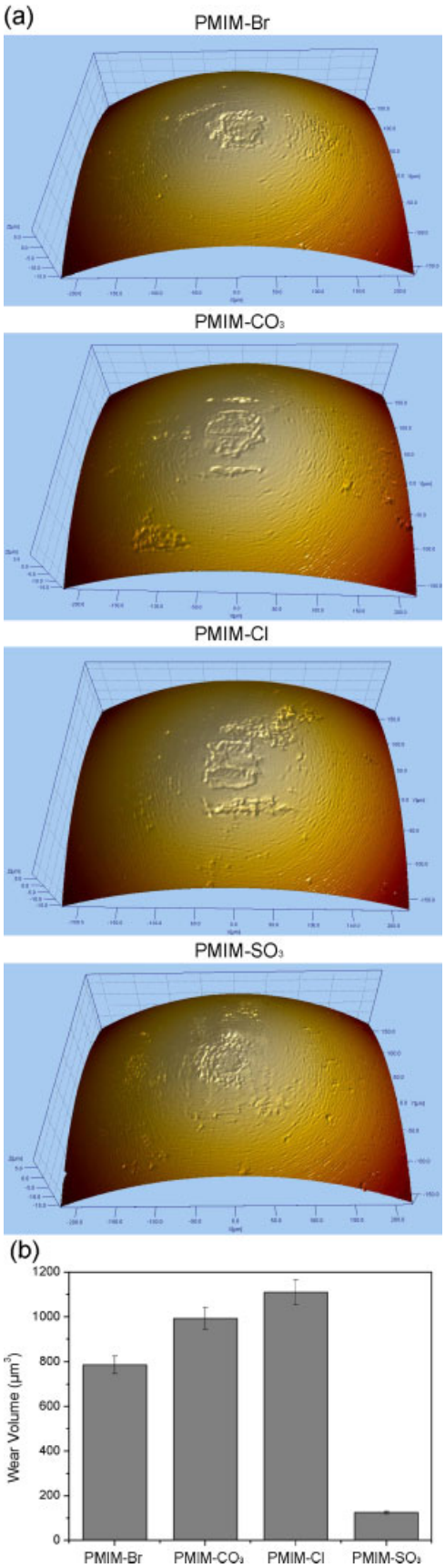

Figure 14. Three-dimensional interferometric microscope images (a) and wear volume (b) of worn surface of the counterpart ball against various films at loads of 60 mN and frequency of 3 Hz for 3600 s.

the wear volume of the counterpart balls against the IL films. The wear volume of PMIM-Br, PMIM-CO_3, PMIM-Cl and PMIM-SO_3 were determined to be about 787, 993, 1109 and 125 μm^3, respectively. PMIM-SO_3 film exhibits a low wear volume compared to PMIM-Br, PMIM-CO_3 and PMIM-Cl. The worn surfaces of IL film and the counterpart ball were examined by X-ray photoelectron spectroscopy measurements after and before the wear test. No obvious chemical shift was observed after the wear test, indicating that there was no chemical change occurring during the friction process and the good tribological performance of IL film was due to the production of new chemical components.

Conclusion

In this work, four kinds of novel ultrathin wear-resistant IL films with thickness ranging from approximately 2 to 70 nm were prepared as uniform coatings by dip-coating methods. Adhesion and friction measurements at the nanoscale were carried out using a colloidal probe. Based on topography, adhesion and friction data, all IL films are found to be prone to attach to the silicon substrate surface, leading to more uniform coatings and lower adhesion and friction. PMIM-Br and PMIM-SO_3 show favorable lubrication as seen from adhesion and friction, which are less than those of PMIM-CO_3, PMIM-Cl and uncoated silicon in all cases. The microscale friction and wear of the four IL films were evaluated at loads ranging from 60 to 300 mN and sliding frequency in range 1–20 Hz. All IL films showed favorable friction reduction and durability. PMIM-Cl and PMIM-CO_3 exhibited a low friction coefficient at a normal load of 200 mN. The PMIM-SO_3 exhibits low friction and anti-wear durability even at high-frequency sliding (20 Hz). The difference between microtribology and macrotribology is mostly caused by their different anti-wear mechanisms. In the microscale, it is surface energy that greatly affects the tribological properties, while in the macroscale the wettability as well as the mobility of the IL on the substrate becomes the decisive factor. Thus, from a tribological point of view, the ILs show strong potential as lubricants for M/NMES because they have desirable thermal and tribological properties.

Acknowledgement

This project was sponsored by the Scientific Research Foundation of GuangXi University (Grant No. XBZ100118).

References

[1] S. Hsu, *J. Metrol. Soc. India* **2007**, *22*, 201.
[2] B. Bhushan, in *Springer Handbook of Nanotribology of Nanotechnology* (2nd edn), Springer Verlag, Heidelberg, Germany, **2007**.
[3] R. E. Sulouffin, B. Bhushan, in *Tribology Issue and Opportunities in MEMS*, Kluwer Academic, Dordrecht, **1998**, p 109.
[4] H. Liu, B. Bhushan, *J. Vac. Sci. Technol. A* **2004**, *22*, 1388.
[5] H. Liu, B. Bhushan, *Ultramicroscopy* **2002**, *91*, 185.
[6] B. Bhushan, A. V. Kulkarni., *Langmuir* **1995**, *11*, 3189.
[7] T. Kasai, B. Bhushan, *J. Vac. Sci. Technol. B* **2005**, *23*, 995.
[8] K. K. Lee, B. Bhushan, D. Hansford, *J. Vac. Sci. Technol. A* **2005**, *23*, 804.
[9] S. M. Hsu, *Tribol. Int.* **2004**, *37*, 553.
[10] Y. Mo, M. Zhu, M. Bai, *Colloids Surf. A* **2008**, *322*, 170.
[11] T. Welton, *Chem. Rev.* **2005**, *9*, 2071.
[12] P. Wasserscheid, W. Keim, *Chem. Int. Ed.* **2000**, *39*, 3772.
[13] J. G. Huddleston, A. E. Visser, W. M. Reichert, H. D. Willauer, G. A. Broker, R. D. Roger, *Green Chem.* **2001**, *3*, 156.
[14] J. Dupont, R. F. Souza, P. A. Z. Suarez, *Chem. Rev.* **2002**, *102*, 3667.

[15] R. D. Roger, K. R. Seddon, *Ionic Liquids: Industrial Applications for Green Chemistry*, *ACS Symposium Series 818*, American Chemical Society, Washington, DC, **2002**.
[16] C. F. Ye, W. M. Liu, Y. X. Chen, L. G. Yu, *Chem. Commum.* **2001**, *1*, 2244.
[17] X. Liu, F. Zhou, Y. Liang, W. Liu, *Tribol. Lett.* **2006**, *23*, 191.
[18] Y. Q. Xia, S. Sasaki, T. Murakami, M. Nakano, L. Shi, H. Z. Wang, *Wear* **2007**, *262*, 765.
[19] P. Bonhote, A. Dias, N. Papageoriou, K. Kalyanasundaram, M. Gratzel, *Inorg. Chem.* **1996**, *35*, 1168.
[20] J. Qu, J. J. Truhan, S. Dai, H. Luo, P. J. Blau, *Tribol. Lett.* **2006**, *22*, 207.
[21] X. Q. Liu, F. Zhou, Y. M. Liang, W. M. Liu, *Wear* **2006**, *261*, 1174.
[22] A. E. Jimenez, M. D. Bernudez, F. J. Carrion, G. M. Nicolas, *Wear* **2006**, *261*, 347.
[23] W. M. Liu, C. F. Ye, Q. Y. Gong, H. Z. Wang, P. Wang, *Tribol. Lett.* **2002**, *13*, 81.
[24] B. Bhushan, M. Palacio, B. Kinzig, *J. Colloid Interface Sci.* **2008**, *317*, 275.
[25] M E V. Valkenburg, R. L. Vaughn, M. Williams, J. S. Wikes, *Thermochim. Acta* **2005**, *425*, 181.
[26] Z. Tao, B. Bhushan, *Wear* **2005**, *259*, 1352.
[27] G. Caporiccio, L. Flabbi, G. Marchionniand, G. T. Viola, *J. Synth. Lubr.* **1989**, *6*, 133.
[28] S. Mori, W. Morales, *Wear* **1989**, *132*, 111.
[29] A. S. Pensado, M. J. P. Comunas, J. Fernandez, *Tribol. Lett.* **2008**, *31*, 107.
[30] V. V. Tsukruk, V. N. Bliznyuk, *Langmuir* **1998**, *14*, 446.
[31] Y. Mo, M. Bai, *J. Phys. Chem. C* **2008**, *112*, 11257.
[32] Y. Mo, Y. Wang, M. Bai, *Phys. E* **2008**, *41*, 146.
[33] X. D. Xiao, L. M. Qian, *Langmuir* **2000**, *16*, 8153.
[34] B. Bhushan, *Handbook of Micro/nano Tribology* (2nd edn), CRC Press, Boca Raton, FL, **1994**.